ASSESSMENT OF EXTERNAL VESSEL COOLING FOR IN-VESSEL RETENTION

K. Atkhen, N. Mérigoux, and J. Lavieville
EDF R&D / MFEE
6 quai Watier 78401 Chatou Cedex, France
kresna.atkhen@edf.fr, nicolas.merigoux@edf.fr; jerome-marcel.lavieville@edf.fr

ABSTRACT

In-vessel retention is among the accident mitigation strategies that are already implemented in several reactors, either operating or under construction. It is also considered for other reactor designs or as a back fitting option. Among others, the success of IVR strategy relies on the capability of the water, surrounding the RPV, to remove the residual heat from the molten core located in the lower vessel plenum. This can be achieved if the local thermal load remains lower than the critical heat flux (CHF) on the external vessel surface.

Such CHF data are usually measured in 1:1 in height experimental facilities, assuming an axisymmetric behavior and simulating real thermal insulation design that creates an optimized streamlined flow path to ensure high CHF values. Nevertheless, most of the heater surface material used in these loops are not made in prototypical vessel steel and therefore it is difficult to extrapolate measured CHF value to reactor situation, as at low pressure, it is well known that surface effects has a strong impact on CHF. It may also be the case with water chemistry that can modify the surface properties of the vessel.

The paper presents a methodology for assessing the limits of coolability which relies on the use of CFD calculations of the thermosiphon around the thermal insulator (using Neptune_CFD code) together with an empirical CHF correlation based on recent experiments at MIT for French and US vessel steel and typical industrial water chemistry. Some results of this methodology are then presented and compared with experimental results, as well as R&D perspectives to strengthen this approach which aim is to be usable in 3D configuration and whatever the reactor design.

KEYWORDS
In-vessel retention, External vessel cooling, Critical Heat Flux

1. INTRODUCTION

In-vessel retention is among the accident mitigation strategies that are already implemented in several reactors, either operating or under construction. It is also considered for other reactor designs or as a back fitting option. Among others, the success of IVR strategy relies on the capability of the water, surrounding the RPV, to remove the residual heat from the molten core located in the lower vessel plenum. This can be achieved if the local thermal load remains lower than the critical heat flux (CHF) on the external vessel surface.

Such CHF data are usually measured in 1:1 in height experimental facilities, assuming an axisymmetric behavior and simulating real thermal insulation design that creates an optimized streamlined flow path to ensure high CHF values. Nevertheless, most of the heater surface material used in these loops are not made in prototypical vessel steel and therefore it is difficult to extrapolate measured CHF value to reactor situation, as at low pressure, it is well known that surface effects has a strong impact on CHF. It may also be the case with water chemistry that can modify the surface properties of the vessel.

The paper presents a methodology for assessing the limits of coolability which relies on the use of CFD calculations of the thermosiphon around the thermal insulator (using Neptune_CFD code) together with an empirical CHF correlation based on recent experiments at MIT for French and US vessel steel and typical industrial water chemistry. As an example, this methodology is applied to AP1000 reactor case, then compared with experimental results.

2. OVERALL METHODOLOGY FOR ASSESSING EXTERNAL VESSEL COOLING

Success of external vessel cooling is achieved if at all time and locations, the local heat flux to the water remains below the CHF. At low pressure (~ atmospheric), there is a significant impact of the surfaces properties of the heater on CHF (vs high pressure flow) on dryout phenomenon. Water chemistry and materials are linked to these surfaces properties. Using 1:1 scale in height loops are necessary for the demonstration as they provide the natural circulation flow characteristics for a given design and a given optimized baffle geometry. However, because of technological issues, these loops often use non prototypical material / water chemistry. Some CHF correlations were built using these large scale loop, but they shall not be extrapolated to any reactor design, as they are design-specific. For example, the different ULPU configurations provided one correlation for each reactor case in the following form: $CHF = K_0 + \Sigma K_i * \Theta^i$ where the different coefficients are linked to specific reactor design (VVER440, AP600, AP1000).
In the approach presented here, the idea is to get a CHF correlation based on experiments under representative conditions but independently from a specific reactor design, and then apply this correlation in CFD post-computations of the external vessel cooling flow. The CFD calculations are done for a specific reactor design, for a specific thermal load and for a specific baffle geometry. At each cell of the fluid domain, the equilibrium quality and superficial velocity of the flow are calculated by CFD computations for every polar angles. A cross-section averaged values for those parameters are injected in the CHF correlation, together with the polar angle. Therefore, as illustrated in the next figure (CEA's SULTAN correlation [1] applied to ULPU loop), for each cell of the mesh (then at different polar angle) it is theoretically possible:

- to assess coolability margins for a given reactor design and a given corium-to-the-vessel heat flux profile;
- but also to experiment numerically new design of baffle shape at "moderate cost" (ie. without having to build a 1:1 scale in height experimental loop) providing that the correlation is used within its validity range.

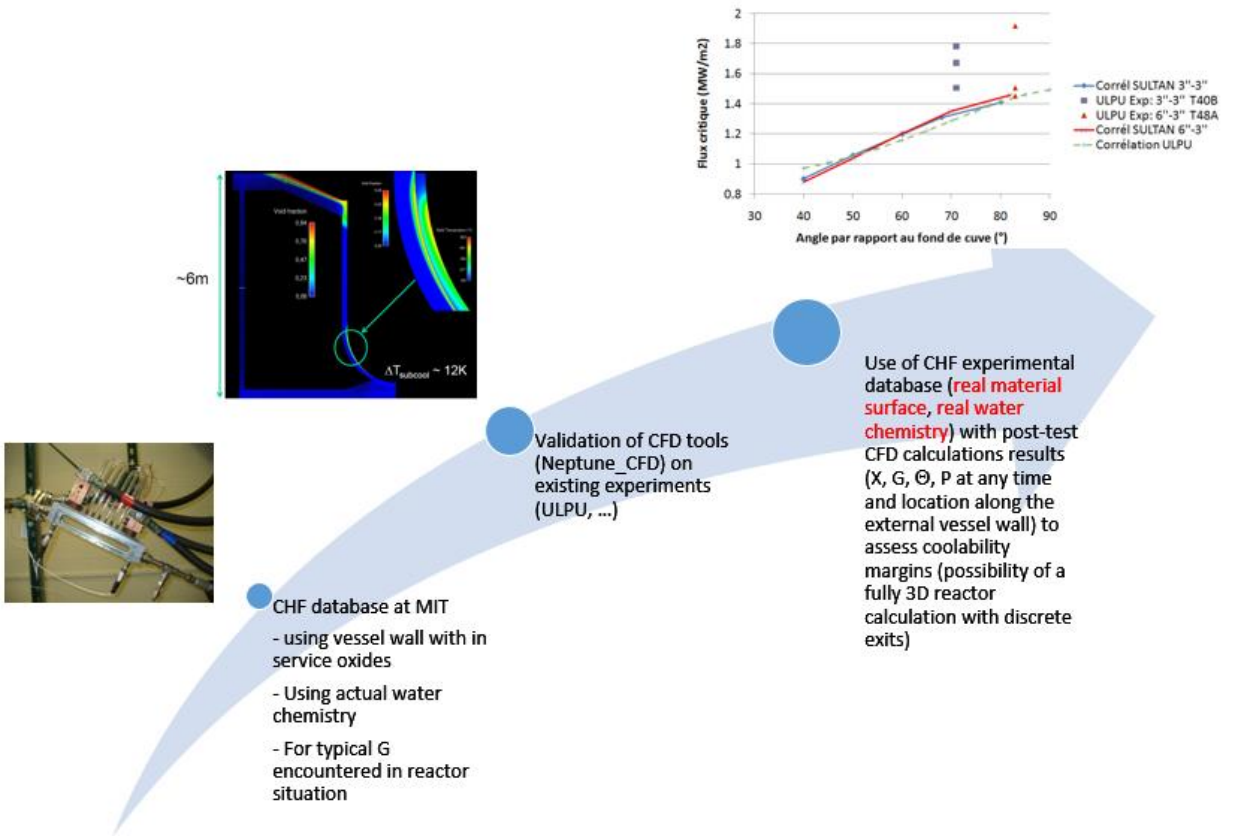

Figure 1. Methodology description

For licensing purposes, industrial feedbacks suggest that these numerical assessments would never replace any 1:1 scale (in height) loop.

However:

- It is difficult at large scale to work with prototypic material / water chemistry. Because of its higher thermal conductivity, copper heaters are generally preferred to simulate reactor vessel wall;
- In such loops, as an axisymmetric flow is always assumed (2D-slice, or 2D-sector designs), the 3D effects (eg. exit conditions of the thermosiphon) cannot be catched. In reactor situation, the flow exits the gap through discrete holes generally located at the main pipes of the primary loop. The upper part of the thermosiphon can be subject to flashing phenomena because of the low water head and low pressure, leading to instabilities and local recirculation or even temporary blockage of the thermosiphon. A full 3D CFD computation may help understanding these 3D effects and hopefully providing some design recommendations, although catching correctly such phenomena is not guaranteed.

3. CRITICAL HEAT FLUX

3.1. UCSB's BETA tests

The BETA tests [2] were performed at the university of California Santa Barbara (UCSB) by Theofanous and Dinh in support to the large scale ULPU V experiments for AP1000 licensing which were done using copper heaters. This experimental program focused on the surface effects and impact of chemicals addition to DI water expected to be present in reactor conditions, namely:

- Tri-Sodium Phosphate (TSP);
- Boric Acid (BA).

Bare prototypical vessel steel surfaces (SA508, equivalent to 16/18MND5), and treated copper surfaces are examined regarding CHF measurement but in pool boiling configuration (no circulating fluid). Using DI water only was to connect with ULPU experimental data with cleansed copper heaters. Prior to CHF measurements, the vessel steel was subjected to a heat treatment at 500°C for a short period). UCSB wrote that this treatment, "*causing steel surface oxidation and aging, mimics thermal conditions the reactor vessel lower head is subjected to during normal reactor operation*".

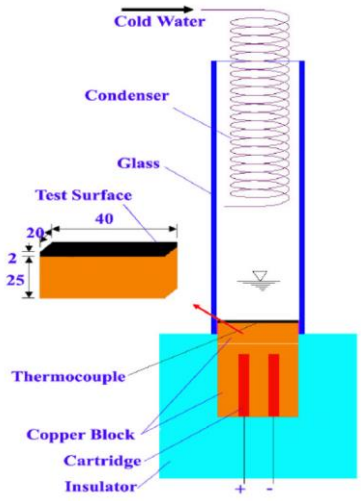

Figure 2. BETA facility (UCSB)

The main conclusions were the following:

- *Effect of surface material and aging by exposure to air and to boiling to all runs made with pure DI water leads to an increase of the CHF* (typically from a low value of ~ 750 kW/m2 to over ~ 1,300 kW/m2 in pool boiling configuration);
- *Diluting the TSP water seems to diminish the performance in steel* but not in copper, but the data in this area are too few for definitive conclusion;
- The TSP produced the highest CHF values yet and this is consistent in both copper and steel surfaces. But this test were done using DI+TSP, without BA;
- For UCSB, there is a hint that BA may interfere with the beneficial effect of TSP, somewhat there is indication that these chemicals, acting principally through deposition processes, may interfere with the beneficial effect of TSP;

- The effect of boiling tap water produces instant ageing of copper surfaces, while it has no effect on the already aged steel surfaces. Using tap water may have cause some deposition on the copper heaters of ULPU affecting its surface (increase of the roughness, etc.). This could explain why in the large scale ULPU loop, the CHF were much higher with TAP water (~1.9 MW/m2) rather than with DI water (~1.3 MW/m2);
- The effect of adding BA to DI water was not clear.

3.2. MIT experimental program on CHF for IVR

3.2.1 Overall objective of MIT-EDF program

The objective was to obtain a contemporary critical heat flux (CHF) correlation, to replace/complement CEA's SULTAN correlation used at EDF. The SULTAN correlation is considered not to be appropriate for in-vessel retention conditions where the reactor pressure vessel cavity would be flooded with water. This is due to the fact that the reactor pressure vessel is made of low carbon steel while the SULTAN correlation is based on an experiment which was carried out: 1/ with stainless steel surfaces; 2/ with de-ionized (DI) water only.

Specifically, the RPV surface has an oxide layer that results from pre-service treatment as well as normal operation. This oxide layer introduces significant changes in surface wettability, porosity, and roughness with respect to an as-fabricated steel surface. It is expected that this oxide layer plays a similar role than nanoparticles deposition, resulting in a enhancement of the critical heat flux [3].

It is also important to have a good representativeness of water chemistry. The experimental matrix considered the addition of boric acid (BA) and tetraborate decahydrate[1] (STB) to the DI water at the following prototypical concentrations:

- 1700 PPM of enriched 10Bo à 37% (or 2500 PPM of BA enriched at 20% of 10Bo);
- STB (Na2B4O7.10H20) at 3.5 kg/m3 of water[2].

Based on literature survey, the influence of BA is unclear, though not significant, and the STB has never been tested.

3.2.2. Surface treatment of samples

The experimental program and its main results is described in [4]. Prior to oxidation treatments, the machined samples were cleaned (with DI-water + acetone) and sandblasted. All heater samples were prepared following the same protocol, including rinsing with DI-water, sandblasting, and rinsing before placing the sample into the tube furnace for oxidation. To try to get the prototypical oxide layers on the outer surface of the pressure vessel characterized by EDF, MIT worked to reproduce the thermal and chemical treatment of a real reactor vessel. This goal can be achieved through 2 phases: a dry oxidation treatment (DO) followed by a wet oxidation (WO) treatment.

[1] In French : tetraborate de soude

[2] STB is used by EDF instead of TSP because of precipitation risks and sumps blockage

The industrial thermal profile was applied for MIT samples, in air, to get an inner layer as close as possible to the actual oxide (see curve below). The maximum temperature of 620°C is a little above the maximum temperature used at UCSB for oxidizing SA508 samples in BETA tests (~500°C).

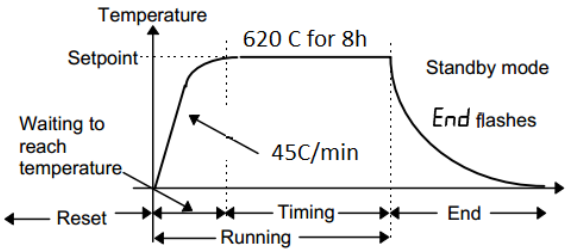

Figure 3. Thermal profile applied to vessel steel samples

The oxidation remained uniform and adherent after sliding the sample out of the furnace. After DO treatment, a WO treatment was conducted to emulate the ambient warm and humid conditions of a reactor pit during service (~300°C at ~70% of humidity, depending on the location of the nuclear power plant during some months/years). To accelerate this process a 100% flowing steam environment was used at MIT but it appeared that it was very difficult to increase this global thickness after a certain time.

When comparing samples treated with DO only, with samples treated with DO+WO, it also appeared that:

- There was no difference on the oxide surface morphology;
- There was no difference on static and dynamic wettability: both samples were super-hydrophilic compared with untreated samples;
- The CHF values with the 2 samples were exactly the same, and far beyond the CHF value with an untreated sample.

As the DO+WO process was very time-consuming, it was decided by EDF and MIT to reproduce only DO oxidation.

3.2.3. Surface structure and wetting properties

As confirmed by confocal microscopy, the surface roughness increases when the oxidation treatment is applied. It is believed that at low pressure, the CHF increases with roughness (though not directly, as increasing roughness increases wettability). It is also well known that there is a strong correlation between a good wettability and a high CHF. Applying the oxidation procedure leads to change the surface structure of the sample. The oxide layer homogeneously covers the entire surface of the heater, and exhibit a "whisker-like" morphology with high opened porosity. Such structures, occurring after 8h of high temperature exposition (620°C) increase wettability. This has been verified by both measuring static and dynamic wettability.

The oxidized surface exhibited super-hydrophilic properties. Static contact angles of the different surfaces are measured using a goniometer to assess the wettability of the treated samples. After oxidation treatment, the contact angle which was initially ~50°, becomes non measurable (~0°).The liquid was also wicked into the heater covering oxide layer. To measure the water absorption ability of an oxidized surface a capillary wicking experiment was set up based on the one reported by [5]. The principle is to

measure the height of water in a normalized capillary tube in contact with the hydrophilic surface and deduce the absorbed volume of water for the oxidized heater as a function of time. The wicking number was then calculated at Wi = 0.52 for the oxidized 18MD5 samples, which according to the model of [5], should result in a CHF enhancement of ~ 55%.

3.3.4. CHF correlation

A straight dimensional correlation was built [4], in the following form:

$$CHF = Y_1\left(\frac{P}{P_c}\right)^{Y_2}\left(\frac{G}{10^3}\right)^{Y_3}\left[1-Y_4\left(\frac{G}{10^3}\right)^{0.5}x_e\right]\left[\frac{3}{2}-\frac{1}{4}\cos(2\theta)\right]$$

- CHF is in MW/m2;
- P denotes the pressure at location of CHF (in bar);
- P_c the critical pressure of water (Pc = 221 bar);
- G is the superficial mass flow rate (kg/m2/s);
- Theta is the orientation angle;
- Y1 = 3.8432; Y2 = 0.1871; Y3 = 0.2999; Y4 = 8.1964.

This correlation is empirical. It is only valid for the following parameters:

- Heater material: French or US oxidized vessel steel (SA508 / 16MND5 /18MND5)
- Coolant: DI water + BA + STB at the following concentrations:
  - ✓ 1700 PPM of enriched 10Bo à 37% (or 2500 PPM of BA enriched at 20% of 10Bo);
  - ✓ 3.5 kg/m3 of Na2B4O7.10H20 diluted in DI water.
- Polar angle theta: from 30° to 90°
- Gap size: 2 cm
- Mass flux (or superficial velocity) G: 350 – 750 kg/m2/s (some additional point were performed at higher values)
- Equilibrium quality Xe: - 0.02 to + 0.02
- Local pressure: 1.03 bar (until 4 bar for polar angle of 90°)

The CHF values at 1.03 bar are bounding values: in reactor situation, it may be higher because of the water level in the cavity and/or if the containment is under pressure.

3.2.5 The gap thickness issue

One remaining issue with this correlation is the gap thickness of the test section used (i.e. the distance between the heated wall and the opposite adiabatic wall). The thickness of the test section should be large enough to let the two-phase boundary layer develop. This is necessary to avoid introducing scale effects, and have a possible extrapolation to large gaps (i.e. gap in reactor situation, which, for AP1000 at a polar angle of 90°, is 6 inches or ~15 cm).

The experimental gap at MIT was 2 cm, and in this current framework it was impossible for MIT to

increase the gap for some few points to check this assessment. This required to fabricate a new test section, a larger pump, and a larger electric supply facility. However, the flow thickness and depth of the test section should be sufficient to eliminate any edge effect: the gap thickness is much larger than the size of individual bubbles, which is the order of the Laplace length (about 2-3 mm). Visual observation of the flow suggests that, at high heat fluxes, the bubble layer generated at the heated wall occupies a significant fraction of the test section flow area. One may think that it is unlikely that interaction between the edge of the bubble layer and the adiabatic wall would affect DNB, which is a very localized phenomenon occurring at the heated wall. Besides, in the SULTAN program, S. Rougé [1] mentioned that "Gap seems to have no effect when CHF is reached for saturated conditions (generally in vertical position)". For mid-size and high power reactor, it is in vertical position (polar angle of ~90°) where the maximum thermal heat flux is expected (focusing effect). The experimental gap in SULTAN was from 3 cm to 15 cm, and the loop principle is the same than in MIT (inclined heated wall, with controlled entry conditions for the coolant). But the SULTAN experiments was done in stainless steel and DI water and rigorously it should be checked using oxidized 16MND5 material with a prototypical water chemistry.

4. NUMERICAL SIMULATIONS

4.1. Model description

The following section will only describe the main principles of the used models. Details on the governing equations of NEPTUNE_CFD have already been extensively described in the literature and will only be summarized in the next paragraph. Next section will be dedicated to the validation and CHF correlation from MIT application steps.

4.1.1 Two-phase model and solver

NEPTUNE_CFD is a three dimensional two-fluid code developed more especially for nuclear reactor applications. This code is based on the classical two-fluid one-pressure approach [7], [8], and is able to simulate multi-component multiphase flows by solving a set of three balance equations for each field [9], [10], [11], [12]. These fields can represent many kinds of multiphase flows: distinct physical components (e.g. gas, liquid and solid particles); thermodynamic phases of the same component (e.g. liquid water and its vapour); distinct physical components, some of which split into different groups (e.g. water and several groups of different bubble diameters); different forms of the same physical components (e.g.: a continuous liquid field, a dispersed liquid field, a continuous vapour field, a dispersed vapour field).The discretization follows a 3D full-unstructured finite-volume approach, with a collocated arrangement of all variables. Numerical consistency and precision for diffusive and advective fluxes for non-orthogonal and irregular cells are taken into account through a gradient reconstruction technique. Convective schemes for all variables, except pressure, are SOLU / upwind scheme. Velocities components can be computed with a SOLU scheme. The solver is based on a pressure correction fractional step approach. Gradients are calculated at second order for regular cells and at first order for highly irregular cells.
A set of local balance equations for mass, momentum and energy is written for each phase. These balance equations are obtained by ensemble averaging of the local instantaneous balance equations written for each phase. When the averaging operation is performed, the major part of the information about the interfacial configuration and the microphysics governing the different types of exchanges is lost. As a consequence, a number of closure relations must be supplied for the total number of equations (the balance equations and the closure relations) to be equal to the number of unknown fields. We can distinguish three different types of closure relations. Those which express the inter-phase exchanges (interfacial transfer terms), those which express the intra-phase exchanges (molecular and turbulent

transfer terms) and those which express the interactions between each phase and the walls (wall transfer terms) [11]. Several turbulence models are available in NEPTUNE_CFD to solve all kind of high-Reynolds multiphase flows. Regarding free surface and dispersed bubbly flows, classical models like k-ε [13] or k-ε "linear production" [14] where available in first versions. A more advanced Reynolds Stress turbulence Model, namely R_{ij}-ε SSG [15], has been introduced and is now extensively used to model highly anisotropic turbulence that is encountered in PWR. The use of its variant, the R_{ij}-ε SSG EBRSM (based on an elliptic blending) [16], for low Reynolds flows or with fine mesh refinements near the wall is now available and of particular interest for applications involving natural convection.
NEPTUNE_CFD inherits the I/O and High Performance Computing capabilities of the EDF open-source CFD software *Code_Saturne* used as a pre-requisite library, can be coupled with the SYRTHES solid-conduction code for conjugate heat transfer and can be used as a module of the SALOME platform.

4.1.2. Generalized Large Interface Model

Separated phases phenomena involve interfaces between liquid and gas which are generally much larger than the computational cells size: the "large interfaces". Specific models to deal with them were developed and implemented in NEPTUNE_CFD: it is the Large Interface Model (LIM) [17]. It includes large interface recognition, interfacial transfer of momentum (due to friction and phase change), heat and mass transfer with Direct Contact Condensation (DCC). The LIM takes into account large interfaces which can be smooth, wavy or rough.
Regarding the interface recognition, the method implemented in NEPTUNE_CFD is based on the gradient of liquid fraction. The first step consists in computing a refined liquid fraction gradient, based on harmonic or anti-harmonic interpolated values of liquid fraction on the faces between the cells [18]. This refined gradient allows us to detect the cells belonging to the Large Interface (LI). The models – specific LI's closure laws – developed and implemented in NEPTUNE_CFD ([19], [20], [21]) are written within a three-cell stencil (LI3C) around the large interface position (including the two liquid and gas neighbouring cells located in LI's normal direction). This stencil is used to compute, on both the liquid and gas sides, the distance from the first computational cell to the large interface. Both distances are used in the models written in a wall law-like format. In this manner, only physically relevant values are used by choosing the interface side where the phase is not residual and the effect of the LI's position with regard to the mesh is limited.
On the other side, a full and closed set of models and closures has been chosen for the simulation of two-phase bubbly flows. It includes the following momentum interfacial transfer closure terms: drag from [22], added mass from [23], turbulent dispersion from in-house "GTD" model [24], lift and wall lubrication forces from Tomiyama [25]. Details about the model implementation in NEPTUNE_CFD are given by [26].
For thermal flow, bulk mass and energy transfer uses Manon-Berne model [27], while bubble nucleation at heated walls uses an extension of the Kurul-Podowski [28] heat partitioning model.
An interfacial area transport equation based on the Ruyer-Seiler polydispersed formulation is solved [29], following the "moment-density" approach, which consists in assuming a certain form for the bubble diameter distribution function (other than a delta Dirac distribution), and then solving equations on the moments defining this distribution. Coalescence and break-up of bubbles are thus systematically taken into account to predict the local bubble sizes.
The Generalized LIM consists in mixing both the large interface and dispersed bubbly flow momentum interfacial closure terms to take full advantage of the previous validation work and development feedback [30]. Using this approach also requires only two fields (one for each phase) which is quite comfortable in terms of CPU time. Furthermore, the model tends towards the dispersed bubbly flow model in area with low void fractions and behaves as the LIM when the mesh is fine enough to capture the large interfaces.

4.2. Validation and CHF correlation application

The following section will now focus on the description of ULPU-V validation case which is representative of an AP1000 reactor and on the application of the CHF correlation developed by MIT. Computation presented below has been performed with the standard version 4.2 of NEPTUNE_CFD, and with a single and consistent set of models (described above), avoiding case-dependent "tuning" of the modelling. We considered a steady-state two-phase, thermal and turbulent flow (R_{ij}-ε SSG,including bubble-induced turbulence production through a source term proportional to the drag force – i.e. assuming that all energy lost by the bubbles due to the drag force is converted into turbulence in the wake of the bubbles), with varying physical properties (depending on the pressure and temperature fields).

4.2.1. Description of the test case

ULPU is an experimental facility at the University of California Santa Barbara designed to assess the coolability limits of an IVR strategy. It was initially set up to perform a program of tests specifically devoted to Lovisaa VVER-440/213 reactor and subsequently modified to assess the Westinghouse AP600 and AP1000 reactors. The facility is a full-scale representation, with respect to height, of a reactor lower head and the whole flow path between the reactor vessel and the reflecting thermal insulation, all the way to the top venting openings. The full-scale height of the flow path (gravity head) is represented for accurate simulation. In addition, vertical slice geometry is used to achieve an effective full-scale simulation of the axisymmetric reactor geometry [31].
Several configurations have been tested. In the first configurations, the facility was capable of generating local heat fluxes of up to 2000 kW/m². The main improvements in ULPU configuration V include the power heating upgrade from 2000 kW/m² to 2 400 kW/m² and the modified curved baffle design with adjustable positioning both at the top and at the bottom of the heated wall. This latest series was used to perform computations with NEPTUNE CFD.
A general view of the loop is provided in **Fig. 4**. Different baffle configurations were employed: for the AP1000 representative configuration, the distance to the vessel varies from 3" at the lowest point of the curved baffle to 6" at the upper-most point of the heater section. The reactor vessel is simulated by copper blocks, with power input provided by embedded cartridge heaters that are individually controlled to allow changing the heat flux shape at will. The blocks are thick enough (7 cm) to simulate the large inertia of the lower head. The width of the slice, imposed by the heater dimensions, is 15 cm.

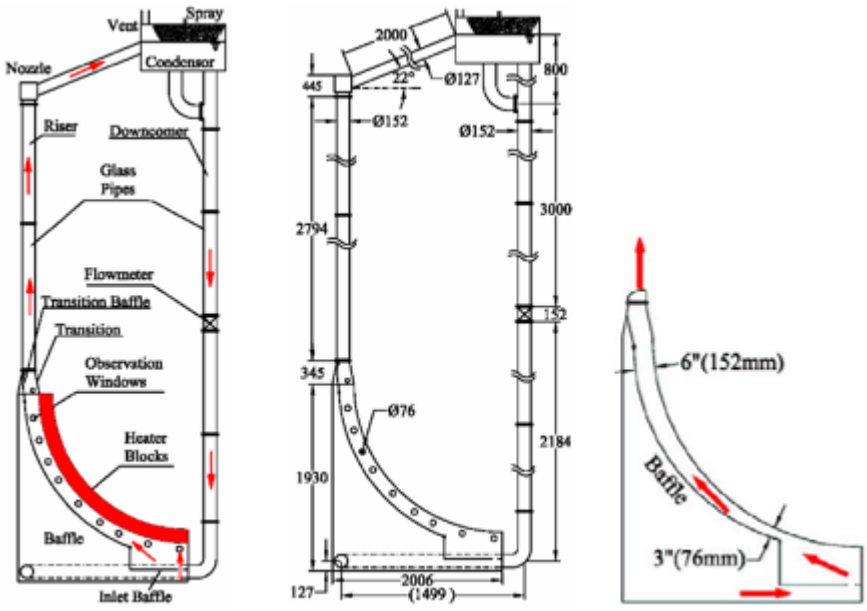

Figure 4. Sketch of the ULPU configuration V facility

An inlet baffle was introduced to represent a similar structure beneath the lowermost region of the lower head (**Fig. 5**). The baffle entry is represented by a 3" hole (76 mm in diameter) yielding 1/84 of the flow areas provided by openings in the inlet baffle incorporated in the AP1000 reactor design. To complete the hot leg of the loop, a riser made of 152 mm diameter glass is used to simulate the full length of the reactor vessel to the top flange. Similarly, in the cold leg, saturated liquid water flows directly from the condenser into the downcomer.

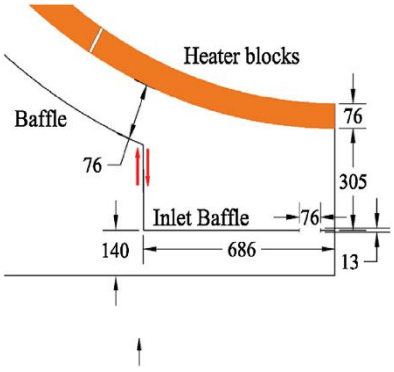

Figure 5. Inlet baffle of the ULPU-V configuration

A total of 36 runs have been carried out on the ULPU-V configurations to evaluate the influence of different parameters such as the baffle geometry, the heat power profile, or the water chemistry. In this article, we will only consider the case with tap water and a 3"-6" baffle geometry which is representative of the AP1000 configuration. The power profiles imposed in the heater blocks is drawn in **Fig. 6**.

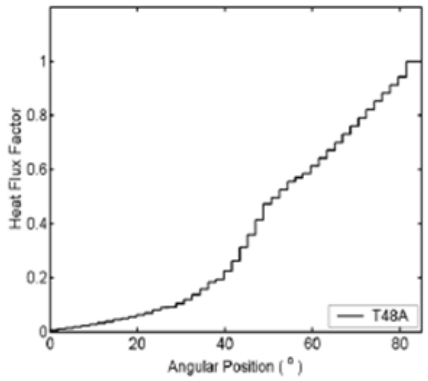

Figure 6. Heat flux profile yielding to a CHF position at 80 – 84°

The water mass flow rate in the downcomer has been measured by an electromagnetic flow meter and will be used for comparisons with NEPTUNE_CFD results.

4.2.2. Computational representation

A 3D approach has been used to model the ULPU-V geometry. The two-phase flow is modelled with NEPTUNE_CFD, while the conjugate heat transfer induced by the heating blocks is taken into account through a code coupling with SYTHES (a thermal conduction code for solids developed by EDF). The computational domain that is used is shown in **Fig. 7**, the red part is the heater blocks modelled with SYRTHES.

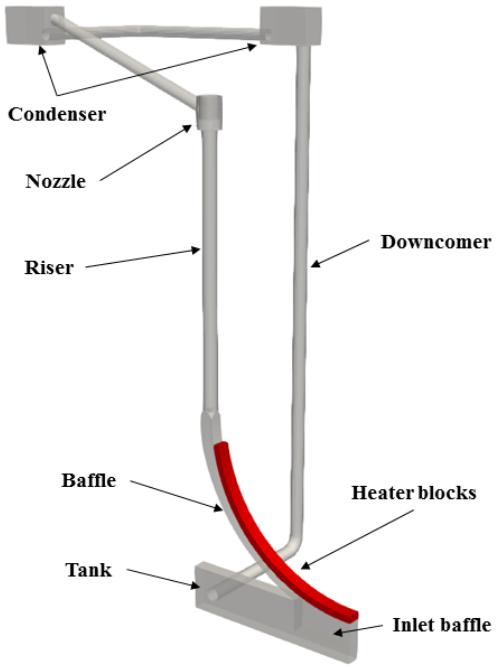

Figure 7. Computational domain used to model ULPU-V configuration

A single mesh refinement, consistent with previous NEPTUNE_CFD validation studies on this test case [31], has been used for this computation. The fluid domain is composed of 300 000 hexa dominant elements (some zones away from the baffle have been meshed with tetrahedrons to ease the meshing process).The corresponding refinement level represents around 10 cells within the baffle gap (Fig. 8).

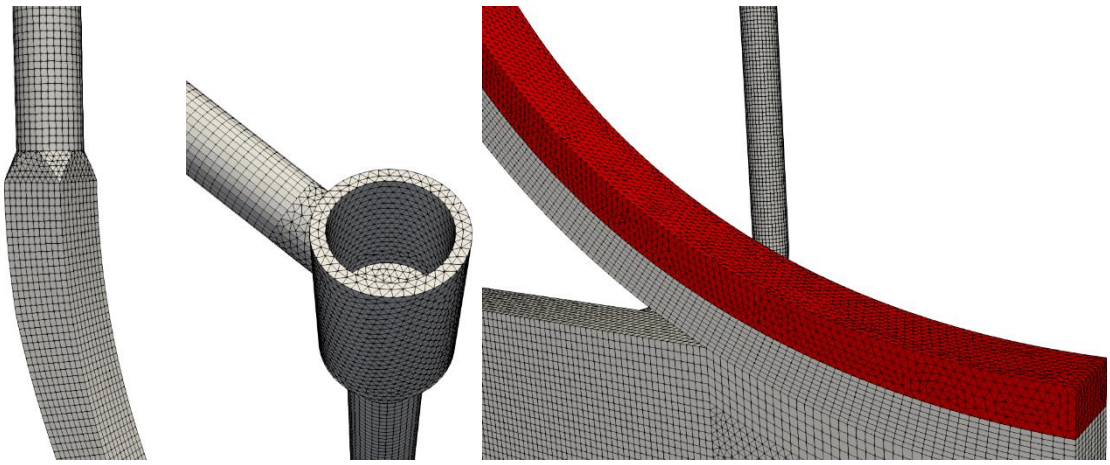

Figure 8. Fluid (grey) and solid (red) mesh of the ULPU-V configuration – zoom on the baffle-riser junction (left), the nozzle (centre) and the baffle-heater blocks junction (right)

Initially, the fluid domain is filled with hot water close to the saturation temperature, and a hydrostatic pressure is imposed (reference pressure of 1 bar on the top of the condenser). Regarding the boundary conditions, free inlet/outlet conditions (with a reference pressure of 1 bar) is located at the top of the condenser. A wall temperature (determined by solving the conjugate heat transfer) is applied where the fluid is coupled with the heater blocks, and a null-flux condition is applied for the remaining adiabatic walls.

4.2.3. Results

The heating generates a driving force for natural circulation, which is balanced by friction losses. Subcooled boiling is the dominant regime near the heated wall. Indeed, the increase of the saturation temperature induced by the significant hydrostatic pressure is not compensated by the power that is provided by the heater blocks. Beyond the upper boundary of the heaters, steam rapidly condenses and coolant flow in the riser becomes essentially single-phase liquid. The coolant boil-off re-emerges at higher elevations, near the nozzle and in the inclined duct by the flashing process (due to a combination of lower saturation temperatures and a singular pressure drop introduced by the nozzle). This void fraction and wall temperature distributions in the loop computed by NEPTUNE CFD are shown in **Fig. 9** (dispersed bubbles corresponding to void fraction below 0.5 are displayed together with contours of continuous gas structures corresponding to void fraction above 0.5).

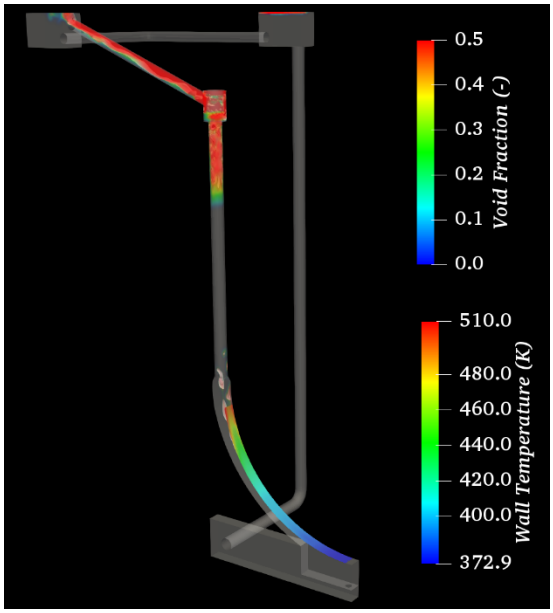

Figure 9. Void fraction and wall temperature distribution in ULPU-V configuration

The water mass flow rate predicted by NEPTUNE_CFD in the downcomer is 0.597 m^3/min, whereas it was experimentally measured to 0.675 m^3/min. It corresponds to around 10% of underestimation error which is quite acceptable when compared with previous studies.

Fig. 10 shows the CHF predictions when using the SULTAN (historically used) and the MIT correlations. It is important to recall that the CHF correlation cannot be extrapolated outside the validation parameters range (typically, above 750 kg/m2/s or below 30° of polar angle). Experimentally, when using ageing copper together with tap water, the CHF value at the angular position of 83° was estimated by UCSB to be 1.9 MW/m². Using NEPTUNE_CFD computational results, the SULTAN correlation provides a CHF value of 1.4 MW/m² (which roughly corresponds to experimental values obtained by UCSB using clean copper and DI water only), while the MIT correlation gives a CHF value of 2 MW/m². As expected, the SULTAN correlation provides conservative results, while the MIT correlation gives a slight overestimation of 10% for the CHF prediction at the angular position of 83°.

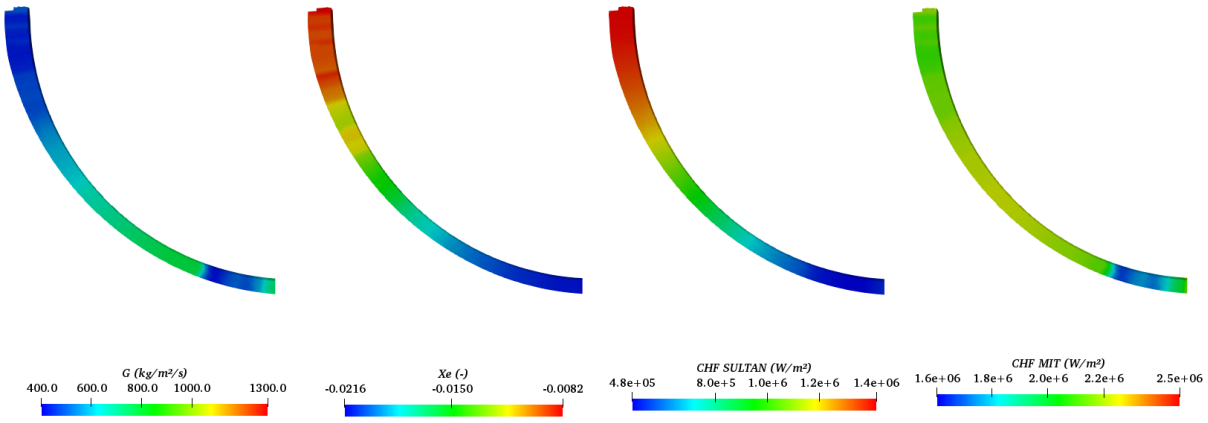

Figure 10. Results for ULPU-V 6-3 configuration: liquid mass flux (left), equilibrium quality (centre-left), SULTAN correlation (centre-right) and MIT correlation (right)

The slight overestimation of CHF prediction with the MIT correlation may be due to the use of different water chemistry and/or metal surface on which nucleate boiling occurs (ageing copper with tap water for ULPU-V experiment and oxidized RPV steel with DI water, BA and STB for MIT experiment). Nevertheless, if one assumes that an ageing copper heater has closer surface characteristics to oxidized vessel steel regarding CHF, especially compared to stainless steel or cleansed copper and as suggested by BETA experimental results, a rather good estimation of the CHF is provided for this configuration representative of the AP1000 by applying the MIT correlation to NEPTUNE_CFD results.

5. CONCLUSIONS

A first reactor application is done using MIT CHF correlation applied to post-tests CFD calculations using NEPTUNE_CFD code. When considering the thermal profile, water chemistry (tap water) and material (ageing copper) that led UCSB to measure the high critical heat flux of 1.9 MW/m^2 at 83° of polar angle, the MIT correlation with the natural circulation flow rate calculated by NEPTUNE_CFD predict a CHF of 2 MW/m^2 which is pretty close. The UCSB's BETA tests have shown in pool boiling geometry the effect of material surface and water chemistry on the CHF. Especially it was observed that ageing by exposure to air and to boiling the surface material to all runs leads to an increase of the CHF. Even if ageing copper is not comparable with oxidized vessel steel, both exhibit higher CHF values compared to stainless steel or cleansed copper.

However, while the SULTAN database suggests a weak dependence of CHF on the gap size, we re-emphasize that the gap size in MIT test section (2 cm) is much lower than that in reactor applications (7–15 cm). Verification of the current CHF correlation at the correct gap size (not possible with the current apparatus) would be highly desirable.

REFERENCES

1. S. Rougé, I. Dor, G. Geffraye "Reactor Vessel External Cooling for Corium Retention - SULTAN experimental Program and Modelling with CATHARE Code", Workshop on in-vessel core debris retention and coolability, Garching , Germany, 3-6 March, 1998
2. CRSS-03/06 June 30, 2003 Limits of Coolability in the AP1000-Related ULPU-2400 Configuration V Facility T-N. Dinh, J.P. Tu, T. Salmassi, T.G. Theofanous, K-NERI program (https://www.nrc.gov/docs/ML0319/ML031920123.pdf)
3. G. DeWitt, T. McKrell, J. Buongiorno, L.W. Hu, R. J. Park "Experimental Study of Critical Heat Flux with Alumina water Nanofluids in Downward Facing Channels for In Vessel Retention Applications", Paper N9P0148,The 9th International Topical Meeting on Nuclear Thermal Hydraulics, Operation and Safety (NUTHOS9), Kaohsiung, Taiwan, September 9-13, 2012
4. M. Trojer, R. Azizian, J. Paras, T. McKrell, K. Atkhen, J. Buongiorno "A margin missed: The effect of surface oxidation on CHF enhancement in IVR accident scenarios" Nuclear Engineering and Design **335** (2018) 140–150
5. O'Hanley, Harry, Carolyn Coyle, Jacopo Buongiorno, Tom McKrell, Lin-Wen Hu, Michael Rubner, and Robert Cohen. "Separate Effects of Surface Roughness, Wettability, and Porosity on the Boiling Critical Heat Flux." Appl. Phys. Lett. **103**, no. 2 (2013): 024102.
6. Rahman, M. M. et al. « Role of Wickability on the Critical Heat Flux of Structured Superhydrophilic Surfaces". Langmuir 30 (37), 11225-11234, septembre 2014
7. M. Ishii, *Thermo-fluid Dynamics Theory of Two-Phase Flow*, Eyrolles, Collection de la direction des Etudes et recherches d'Electricité de France, 1975.
8. J.-M. Delhaye, M. Giot, M.L. Riethmuller, *Thermal-hydraulics of two-phase systems for industrial design and nuclear engineering*, Hemisphere and McGraw Hill, 1981.
9. N. Méchitoua et al., "An unstructured finite volume solver for two-phase water/vapor flows modelling based on an elliptic-oriented fractional step method", *Proc. NURETH-10*, Seoul, October 5 – 9 2003.
10. A. Guelfi, D. Bestion, M. Boucker, P. Boudier, P. Fillion, M. Grandotto, J.-M. Hérard, E. Hervieu, P. Péturaud, "NEPTUNE - A New Software Platform for Advanced Nuclear Thermal-Hydraulics", *Nuclear Science and Engineering*,**156**,281-324 (2007).
11. S. Mimouni, F. Archambeau, M. Boucker, J. Laviéville, C. Morel, "A second order turbulence model based on a Reynolds stress approach for two-phase boiling flow. Part 1: Application to the ASU-annular channel case", *Nuclear Engineering and Design,* (2009a).
12. S. Mimouni, F. Archambeau, M. Boucker, J. Laviéville, C. Morel, "A second order turbulence model based on a Reynolds stress approach for two-phase boiling flow. Part 1: Adiabatic cases", *Science and Technology of Nuclear Installations*,**792395**,14 (2009b).
13. B.E. Launder, D.B. Spalding, "The numerical computation of turbulent flows", *Computer Methods in Applied Mechanics and Engineering,* **3**,269-289 (1974).
14. V. Guimet, D. Laurence, "A linearised turbulent production in the k-ε model for engineering applications", *Proc. 5th International Symposium on Engineering Turbulence modelling and measurements*, Mallorca, September 2002.

15. C.G. Speziale, S. Sarkar, T.B. Gatski, "Modelling the pressure-strain correlation of turbulence: an invariant dynamical systems approach", *Journal of Fluid Mechanics,* **227**,245-272 (1991).
16. R. Manceau, "An improved version of the elliptic blending model: application to non-rotating and rotating channel flows", *Proc. 4th International Symposium on Turbulence and Shear Flow Phenomena*, Williamsburg, June 27-29 2005.
17. P. Coste, "A Large Interface Model for two-phase CFD", *Nuclear Engineering and Design*,**255**,38-50 (2013).
18. J. Laviéville, P. Coste, "Numerical modeling of liquid-gas stratified flows using two-phase Eulerian approach", *Proc. 5th International Symposium on Finite Volumes for Complex Applications,* Aussois, June 8 – 13 2008.
19. P. Coste, J. Pouvreau, C. Morel, J. Laviéville, M. Boucker, A. Martin, "Modeling turbulence and friction around a large interface in a three-dimension two-velocity eulerian code", *Proc. NURETH-12,* Pittsburgh, September 30 – October 4 2007
20. P. Coste, J. Pouvreau, J. Laviéville, M. Boucker, "A two-phase CFD approach to the PTS problem evaluated on COSI experiment", *Proc. ICONE 16,*Orlando, May 11 – 15 2008.
21. P. Coste , J. Laviéville, "A Wall Function-Like Approach for Two-Phase CFD Condensation Modeling of the Pressurized Thermal Shock", *Proc. NURETH-13,*Kanazawa, September 27 – October 2 2009.
22. M. Ishii, "Two-fluid model for two-phase flow", *Multiphase Science and Technology*, **5**, 1-58 (1990).
23. N. Zuber, "On the dispersed two-phase flow in the laminar flow regime", *Chemical Engineering Science*, **19**, 897 (1964).
24. J. Laviéville, N. Mérigoux, M. Guingo, C. Baudry, S. Mimouni, "A Generalized Turbulent Dispersion Model for Bubbly Flow Numerical Simulation in NEPTUNE_CFD", *Proc. NURETH-16,* Chicago, August 30 – September 14 2015.
25. A. Tomiyama, "Struggle with computational bubble dynamics", Proc. *3rd International Conference on Multiphase Flow*, Lyon, June 8 – 12 1998.
26. S. Mimouni, C. Baudry, M. Guingo, M. Hassanaly, J. Laviéville, N. Méchitoua, N. Mérigoux, "Combined Evaluation of Bubble Dynamics, Polydispersion Model and Turbulence Modelling for Adiabatic Two-Phase Flow", *Proc. NURETH-16,* Chicago, August 30 – September 14 2015.
27. E. Manon, "Contribution à l'analyse et à la modélisation locale des écoulements bouillants sous-saturés dans les conditions des Réacteurs à Eau sous Pression", *PhD thesis*, Ecole Centrale Paris, (2000).
28. N. Kurul, M.Z. Podowski, "Multidimensional effects in forced convection subcooled boiling", *Proc. of the 9th International Heat Transfer Conference*, Jerusalem, August 19 – 24 1990.
29. P. Ruyer, N. Seiler, M. Beyer, F.P. Weiss, "A bubble size distribution model for the numerical simulation of bubbly flows", *Proc. of 6th International Conference on Multiphase Flows*, Leipzig, July 9 – 13 2007.
30. N. Mérigoux, J. Laviéville, S. Mimouni, M. Guingo, C. Baudry, "A Generalized Large Interface to Dispersed Bubbly Flow Approach to model Two-Phase Flows in Nuclear Power Plant", *Proc. CFD4NRS-6,* Cambridge, September 13 – 15 2016.
31. M. Jamet, J. Lavieville, K. Atkhen, N. Mechitoua, "Validation of NEPTUNE_CFD on ULPU-V experiments", *Nuclear Engineering and Design*,**293**, 468-475 (2015).